

# Threshold displacement energies and displacement cascades in 4H-SiC: Molecular dynamic simulations

Cite as: AIP Advances 9, 055007 (2019); <https://doi.org/10.1063/1.5093576>

Submitted: 22 February 2019 . Accepted: 29 April 2019 . Published Online: 08 May 2019

Weimin Li, Lielin Wang, Liang Bian, Faqin Dong, Mianxin Song, Jianli Shao, Shuqing Jiang, and Hui Guo



View Online



Export Citation



CrossMark

## ARTICLES YOU MAY BE INTERESTED IN

Modification of strain and optical polarization property in AlGaIn multiple quantum wells by introducing ultrathin AlN layer

AIP Advances 9, 055004 (2019); <https://doi.org/10.1063/1.5091027>

Bilayer tunneling field effect transistor with oxide-semiconductor and group-IV semiconductor hetero junction: Simulation analysis of electrical characteristics

AIP Advances 9, 055001 (2019); <https://doi.org/10.1063/1.5088890>

Highly efficient p-type doping of GaN under nitrogen-rich and low-temperature conditions by plasma-assisted molecular beam epitaxy

AIP Advances 9, 055008 (2019); <https://doi.org/10.1063/1.5089658>

## AVS Quantum Science

Co-published with AIP Publishing



Coming Soon!



# Threshold displacement energies and displacement cascades in 4H-SiC: Molecular dynamic simulations

Cite as: AIP Advances 9, 055007 (2019); doi: 10.1063/1.5093576

Submitted: 22 February 2019 • Accepted: 29 April 2019 •

Published Online: 8 May 2019



Weimin Li,<sup>1</sup> Lielin Wang,<sup>1</sup> Liang Bian,<sup>2</sup> Faqin Dong,<sup>2</sup> Mianxin Song,<sup>2</sup> Jianli Shao,<sup>3</sup> Shuqing Jiang,<sup>4,a)</sup> and Hui Guo<sup>5,a)</sup>

## AFFILIATIONS

<sup>1</sup>Fundamental Science on Nuclear Wastes and Environmental Safety Laboratory, Southwest University of Science and Technology, Mianyang 621010, China

<sup>2</sup>Laboratory of Solid Waste Treatment and Resource Recycle, Ministry of Education, Southwest University of Science and Technology, Mianyang 621010, China

<sup>3</sup>State Key Laboratory of Explosion Science and Technology, Beijing Institute of Technology, Beijing 100081, China

<sup>4</sup>Institute of Nuclear Physics and Chemistry, China Academy of Engineering Physics, Mianyang 621900, China

<sup>5</sup>Key Laboratory of Wide Band-Gap Semiconductor Materials and Devices, School of Microelectronics, Xidian University, Xian 710071, China

<sup>a)</sup>Corresponding author: jsq@cqu.edu.cn (Shuqing Jiang); guohui@mail.xidian.edu.cn (Hui Guo)

## ABSTRACT

Molecular dynamic (MD) simulations were used to study threshold displacement energy (TDE) surface and Si displacement cascades in 4H-SiC system. To figure out the role of different Wyckoff sites in determining the TDE values, both Si and C atoms in 2a and 2b Wyckoff sites were separately considered as the primary knocked atoms (PKA). The initial kinetic energy was then distributed along 146 different crystallographic directions at 10 K. TDE surface appeared highly anisotropic for Si and C displacements along different crystallographic directions. The TDE was determined as 41 eV for Si and 16 eV for C. The average values of TDE over two Wyckoff sites were estimated to 66 eV for Si PKA and 24 eV for C PKA. The displacement cascades produced by Si recoils of energies spanning varied from 5 keV to 50 keV at 300 K. To count the number of point defects using Voronoi cell analysis method, the crystal structure of 4H-SiC was transformed from hexagonal to orthorhombic. It was found that the surviving defects at the end of cascades were dominated by C vacancies and interstitials due to low displacement energies of C atoms and greater number of C interstitials when compared to C vacancies.

© 2019 Author(s). All article content, except where otherwise noted, is licensed under a Creative Commons Attribution (CC BY) license (<http://creativecommons.org/licenses/by/4.0/>). <https://doi.org/10.1063/1.5093576>

## I. INTRODUCTION

Silicon carbide (SiC) is an important semiconductor with wide application prospects in high temperature, frequency, and power microelectronic devices. This is mainly due to its wide band gap, high breakdown voltage, and elevated saturation electron mobility.<sup>1,2</sup> SiC is also an important structural material with superior thermal conductivity, chemical inertness, irradiation resistance, and small neutron capture cross section enabling it withstand high flux neutron irradiation in nuclear reactors.<sup>3-6</sup>

SiC-based materials, such as SiC/SiC composites have been utilized as important fuel pellet-cladding layer in high-temperature gas cooled reactors, as well as critical elements in preventing the release of radioactive products.<sup>7-9</sup>

During the process of energetic particles irradiation, SiC lattice produces large numbers of defects. These lead to degradation of its physical, chemical and mechanical properties, which, in turn, directly determine the feasibility and reliability of SiC in anti-irradiation fields. Therefore, it is very important to understand the mechanisms behind defect creation and accumulation.

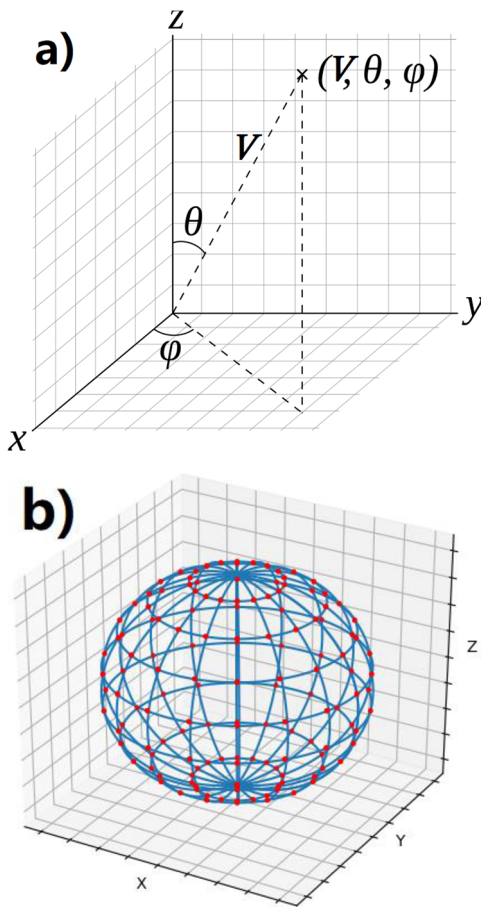


**FIG. 1.** PKA directions in the spherical coordinate system ( $0^\circ \leq \theta \leq 180^\circ$ ,  $0^\circ \leq \phi < 360^\circ$ , and the angle-interval was  $20^\circ$ ).

One basic parameter associated with defect generation deals with threshold displacement energy (TDE), defined as the minimum kinetic energy required to transfer the atom from its lattice to stable Frenkel pairs.<sup>10</sup> Because SiC exhibits polytypism of more than

100 known polytypes, TDE for each polytype should be different from others due to variations in structures and atom arrangements. For instance, Devanathan *et al.*<sup>11</sup> determined the minimum displacement energies of C and Si in 3C-SiC system as respectively 21 eV and 36 eV along 26 different crystallographic directions, as well as 24 eV and 35 eV in 6H-SiC system along 6 directions. However, TDE in 4H-SiC encounters uncertainty. On the other hand, at the exception of 2H-SiC and 3C-SiC systems, other SiC polytypes possess two or more Wyckoff sites for Si or C atoms. Hence, the TDE of each Wyckoff site along the same crystallographic direction should be different due to variations in atomic arrangements.

In this paper, molecular dynamic (MD) simulations were employed to evaluate defect production and evolution. First, TDE of Si and C atoms in 4H-SiC along 26 different crystallographic directions were performed. The displacement cascades produced by Si-recoils at energies spanning from 5 to 50 keV were then simulated at 300 K.

## II. SIMULATIONS

Molecular dynamic (MD) simulations were performed using LAMMPS code.<sup>12</sup> The interatomic interactions were previously described by Tersoff/ZBL empirical potentials.<sup>13</sup> To compute the TDE in 4H-SiC system, cell units with sizes of  $20 \times 20 \times 6$  (equivalent to 19,200 atoms) with periodic boundary conditions were employed. The initial structure was equilibrated in canonical (NVT) ensemble for 15 ps followed by microcanonical (NVE) ensemble for 10 ps. The system temperature was set to 10 K and atom located in the cell centre was selected as primary knocked atom (PKA). The initial kinetic energy was then set along 146 different crystallographic directions in the spherical coordinate system (Fig. 1). The TDE is the minimum energy to displace an atom from its original lattice site to a defect position.<sup>10</sup>

For displacement cascade simulations in 4H-SiC system, Voronoi cell analyses were utilized to identify the defect type and amount of point defect. Because Voronoi cell analysis method was found unsuitable for hexagonal structures, 4H-SiC crystal structure was transformed from hexagonal to orthorhombic. The transformation in crystal structure is shown in Fig. 2. The primary hexagonal unit cell parameters in Fig. 2(i) were set as follows:  $a = b = 3.0815 \text{ \AA}$ ,

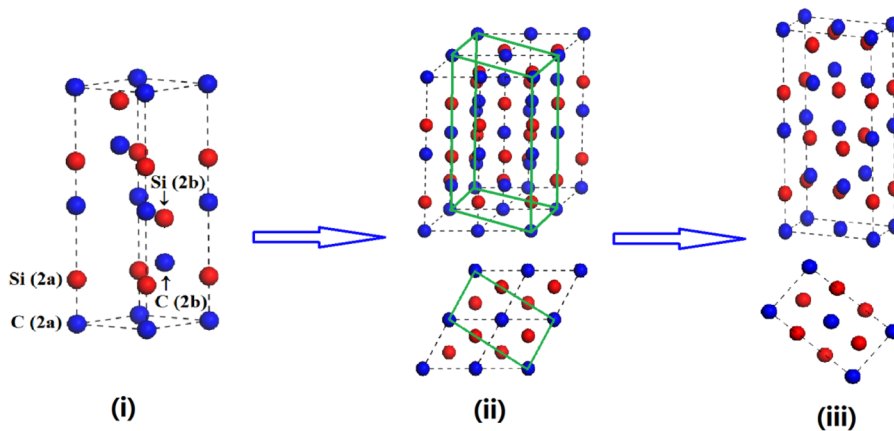


**FIG. 2.** The transformation of crystal structure from hexagonal to orthorhombic in 4H-SiC system. (i) Hexagonal system unit cell with 8 atoms, (ii) hexagonal system  $2 \times 2 \times 1$  unit cells with 32 atoms, and (iii) orthorhombic system unit cell with 16 atoms.

$c = 10.0614 \text{ \AA}$ ,  $\alpha = \beta = 90^\circ$ , and  $\gamma = 120^\circ$ . The transformed orthorhombic unit cell parameters in Fig. 2(iii) were:  $a = 3.0815 \text{ \AA}$ ,  $b = 5.3373 \text{ \AA}$ ,  $c = 10.0614 \text{ \AA}$ , and  $\alpha = \beta = \gamma = 90^\circ$ . The Si-C bond length before and after transformation remained the same ( $1.8870 \text{ \AA}$ ).

The system size of  $250 \times 150 \times 75$  for orthorhombic unit cells (equivalent to 45,000,000 atoms) was used in displacement cascade simulations. At 300 K, the primary super cell was equilibrated in NVT and NVE ensembles for 15 ps and 10 ps, respectively. In displacement cascade simulations, an Si atom located in the cell centre with PKA kinetic energy ranging from 5 to 50 keV in the direction close to  $[1\ 3\ 5]$  was selected with NVE ensembles. Our cascades simulations were based on multiple-phase timestep procedure as previously described.<sup>14</sup> The total simulation time was set to 11.2 ps.

### III. RESULTS AND DISCUSSION

The Wyckoff sites and atomic coordinates of Si and C atoms in 4H-SiC system are summarized in Table I.<sup>15</sup> The Si or C atoms were found located in the 2a and 2b Wyckoff sites, respectively. Due to variations in atomic arrangements in different Wyckoff sites, the TDE in 2a Wyckoff site must be different from 2b Wyckoff site in the same crystallographic direction. Here, TDE in 2a and 2b Wyckoff sites were computed for Si and C atoms.

To compute TDE, an atom should be selected as PKA. After attributing a kinetic energy to the selected atom, it should leave its primary equilibrium location and move along some crystallographic directions. If PKA energy was not high enough, it should return to its original position after relaxation without creating any defects. Until reaching high enough energy, PKA should permanently be displaced from its lattice site to defect position to form at least one stable Frenkel pair.

TDE is prominently dependent on the crystallographic direction. However, the Wyckoff site would significantly impact the TDE. For same type of atoms and crystallographic directions, the resulting TDE should be different due to variation in Wyckoff sites. For this reason, two Wyckoff sites (2a and 2b) were considered for Si and C atoms in 4H-SiC system. The TDE values of two opposite crystallographic directions ( $[0\ 0\ 0\ 1]$  and  $[0\ 0\ 0\ \bar{1}]$ ) were then computed, and the results are gathered in Fig. 3.

For Si atom in 2a site, the TDE was estimated to 101 eV along the  $[0\ 0\ 0\ \bar{1}]$  direction, suggesting the challenging deviation of Si PKA from its equilibrium position due to the repulsive forces exerted by the carbon atom on top of silicon-carbon tetrahedron. On the other hand, TDE changed significantly with a  $180^\circ$  rotation to yield 57 eV along  $[0\ 0\ 0\ 1]$  direction. The latter was attributed to the repulsive forces exerted by the three C atoms on the bottom

of silicon-carbon tetrahedron. The same situation occurred in 2b site for Si atom. The TDE value was calculated as 42 eV along the  $[0\ 0\ 0\ 1]$  direction, which was lower than the 80 eV obtained along  $[0\ 0\ 0\ \bar{1}]$  direction. However, using the same crystallographic direction ( $[0\ 0\ 0\ 1]$  or  $[0\ 0\ 0\ \bar{1}]$ ), the TDE values of various Wyckoff sites looked different because of the asymmetry in atomic arrangements. The C PKA showed the opposite situation, with TDE value along  $[0\ 0\ 0\ 1]$  direction higher than that of  $[0\ 0\ 0\ \bar{1}]$  direction for both 2a and 2b sites. This indicated that the atom located on top of tetrahedron had greater repulsive forces than those of three atoms positioned on the bottom. Also, C PKA could easily deviate from its equilibrium position in the center of tetrahedron when compared to Si PKA.

The average value of TDE is also important because it determines the concentration of defects upon irradiation of the material with large numbers of energetic particles.<sup>16</sup> The present simulations indicated that through TDE of Si PKA along the same crystallographic direction in 2a site was different from that in 2b site, the average TDE values were similar for two Wyckoff sites along more than 146 crystallographic directions. In particular, about 67 eV was estimated for 2a site and 65 eV for 2b site. For C PKA, the average TDE values was about 22 eV for 2a and 26 eV for 2b site. Overall, this may suggest that the average values of TDE may be similar for homogeneous atoms in different Wyckoff sites. Hence, the average TDE values for both Wyckoff sites for 4H-SiC system were determined as 66 eV for Si and 24 eV for C, lower than the 73 eV reported for Si and 37 eV for C in 3C-SiC system, as well as 75 eV for Si and 31 eV for C in 6H-SiC.<sup>11</sup>

In order to statistical analysis of TDE along different crystallographic direction, Thomas *et al.*<sup>19</sup> defined TDE as a function of defect formation probability (DFP). Subsequently, for a more mathematical approach to defining TDE, Robinson *et al.*<sup>20</sup> gave a fit function:

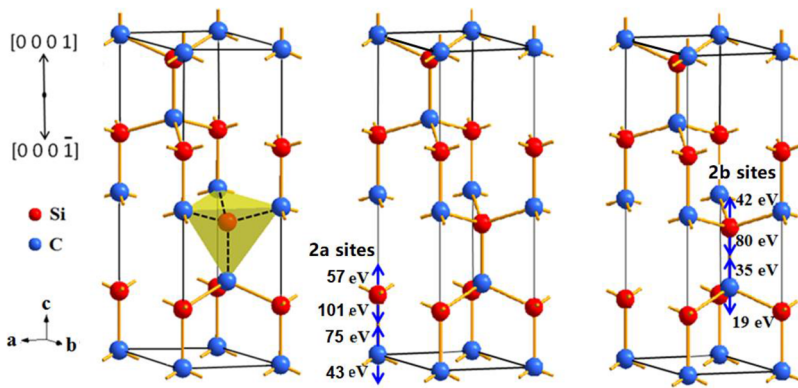
$$\text{DFP}(E) = \begin{cases} 0 & E \leq TDE \\ \frac{1}{\beta} [E^\alpha - (TDE)^\alpha] & E > TDE \end{cases} \quad (1)$$

Where  $\alpha$  and  $\beta$  are fitting parameters and  $E$  is the PKA energy. The fitting result is shown in Fig. 4 and generates Si values of 41.5 eV, 0.104 and 0.097 and C values of 16.43 eV, 0.761 and 6.268 for TDE,  $\alpha$  and  $\beta$  respectively. The DFP of 10% in energies are 44 eV for Si and 18 eV for C. These results show that the DFP for 4H-SiC is significantly less than several oxides such as  $\text{TiO}_2$ ,  $\text{SiO}_2$ ,  $\text{Cr}_2\text{O}_3$ ,  $\text{Al}_2\text{O}_3$  and  $\text{MgO}$ .<sup>20,21</sup>

The defects as a function of time at 10 and 50 keV cascades in 4H-SiC system are depicted in Fig. 5. The point defects in SiC consisted of vacancies ( $V_{\text{Si}}$  and  $V_{\text{C}}$ ) and interstitials ( $I_{\text{Si}}$  and  $I_{\text{C}}$ ), as well as antisites of Si on C site ( $\text{Si}_{\text{C}}$ ), C on Si site ( $\text{C}_{\text{Si}}$ ), Si on Si site ( $\text{Si}_{\text{Si}}$ ), and C on C site ( $\text{C}_{\text{C}}$ ). Here,  $\text{Si}_{\text{Si}}$  ( $\text{C}_{\text{C}}$ ) sites are regarded as Si (C) atoms moving to different positions of Si (C) sublattice. Time dependence of the number of point defects would follow two trends. The first consisted of vacancies and interstitials defects, such as  $V_{\text{Si}}$ ,  $V_{\text{C}}$ ,  $I_{\text{Si}}$  and  $I_{\text{C}}$ , with maximum disorder peak. At the beginning of cascade, a rapid buildup of defects would occur until reaching a maximum number (maximum disorder peak) at around .1 - .3 ps. During subsequent relaxation, defect recovery will occur to decrease the number of point defects followed by a stable state after about 1 ps. The second consisted of antisites, such as  $\text{Si}_{\text{C}}$ ,  $\text{C}_{\text{Si}}$ ,  $\text{Si}_{\text{Si}}$  and  $\text{C}_{\text{C}}$ , where no obvious maximum

**TABLE I.** Structure parameters of 4H-SiC system.<sup>15</sup> Hexagonal, Space group:  $P6_3/mc$  (No. 186).  $a = b = 3.0815 \text{ \AA}$ ,  $c = 10.0614 \text{ \AA}$ ,  $\alpha = \beta = 90^\circ$ , and  $\gamma = 120^\circ$ .

| Atom | Wyc. | x      | y      | z      | Occ. |
|------|------|--------|--------|--------|------|
| Si1  | 2a   | 0.0000 | 0.0000 | 0.1875 | 1.0  |
| Si2  | 2b   | 0.3333 | 0.6667 | 0.4375 | 1.0  |
| C1   | 2a   | 0.0000 | 0.0000 | 0.0000 | 1.0  |
| C2   | 2b   | 0.3333 | 0.6667 | 0.2599 | 1.0  |

FIG. 3. TDE values along  $[0\ 0\ 0\ 1]$  and  $[0\ 0\ 0\ \bar{1}]$  directions.

disorder peak was observed. The number of point defects gradually increased then remained stable after roughly 1 ps. As previously reported,<sup>14,17,18</sup> carbon defects (vacancies and interstitials of C) predominated at both 10 and 50 keV cascades. Obviously, the C vacancies and interstitials were higher than Si vacancies and interstitials observed at the end of simulations. The latter was associated with the lower displacement energies, which made the C atoms easy to leave their equilibrium positions to move towards the interstitial sites.

At 10 keV cascade, the number of both of vacancies and interstitials for C reached the maximum at roughly .1 ps and then the number decreased to ~55% after roughly 1 ps. At 50 keV cascade, the ratio increased to reach ~74% of the original number. Unlike carbon defects, only ~28% and ~38% of the original number for Si vacancies were left at 10 keV cascade. At 50 keV cascade, only ~12% and ~23% of Si vacancies were left for Si interstitials.

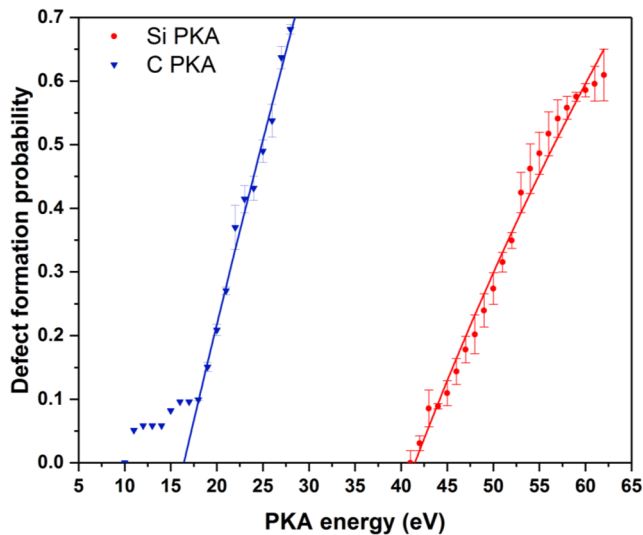


FIG. 4. Defect formation probabilities for both Si and C PKA.

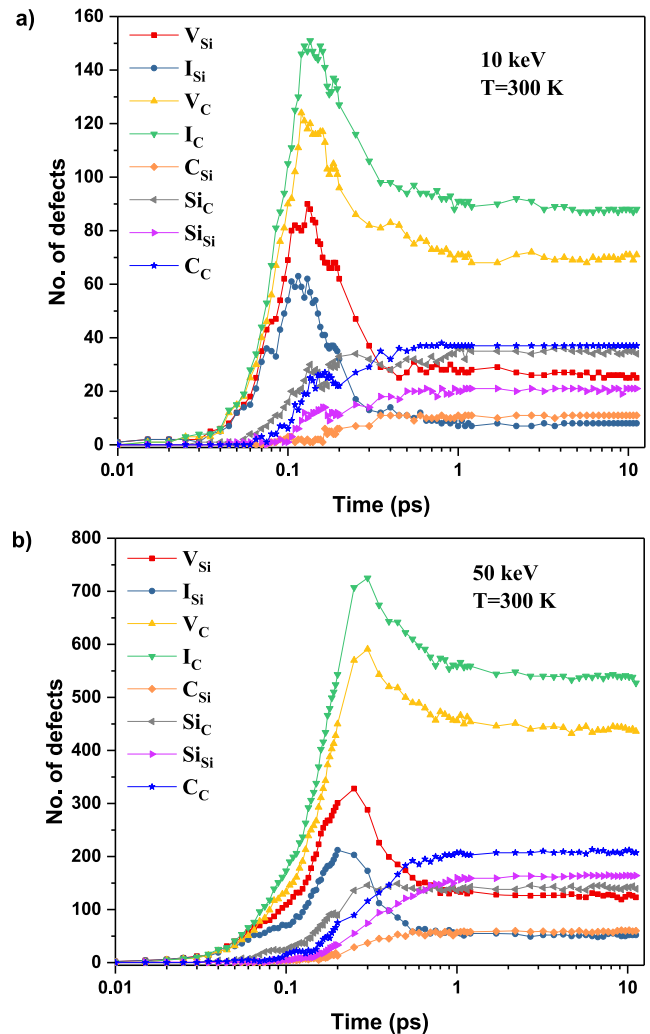


FIG. 5. Time dependence of number of point defects observed in MD displacement cascade simulations at 300 K: (a) 10 keV and (b) 50 keV.



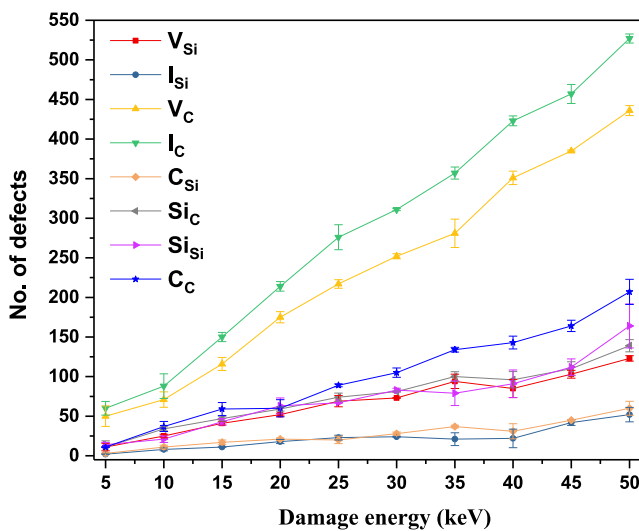


FIG. 6. Damage energy as a function of number of point defects for Si recoils at 300 K.

This suggested that most C vacancies and interstitials were immobilized. The other part of C vacancies were occupied by Si or C atoms to form  $\text{Si}_\text{C}$  ( $\text{V}_\text{C} + \text{I}_\text{Si} \rightarrow \text{Si}_\text{C}$ ) or  $\text{C}_\text{C}$  ( $\text{V}_\text{C} + \text{I}_\text{C} \rightarrow \text{C}_\text{C}$ ) through vacancy-interstitial complex reactions. On the other hand, the C interstitials could move into the Si or C vacancies to induce  $\text{C}_\text{Si}$  ( $\text{I}_\text{C} + \text{V}_\text{Si} \rightarrow \text{C}_\text{Si}$ ) or  $\text{C}_\text{C}$  ( $\text{I}_\text{C} + \text{V}_\text{C} \rightarrow \text{C}_\text{C}$ ). However, only few vacancies and interstitials of Si were immobilized, and most of Si vacancies were occupied by Si or C atoms to form  $\text{Si}_\text{Si}$  ( $\text{V}_\text{Si} + \text{I}_\text{Si} \rightarrow \text{Si}_\text{Si}$ ) or  $\text{C}_\text{Si}$  ( $\text{V}_\text{Si} + \text{I}_\text{C} \rightarrow \text{C}_\text{Si}$ ). Also, the Si interstitials might move into Si or C vacancies to form  $\text{Si}_\text{Si}$  ( $\text{I}_\text{Si} + \text{V}_\text{Si} \rightarrow \text{Si}_\text{Si}$ ) or  $\text{Si}_\text{C}$  ( $\text{I}_\text{Si} + \text{V}_\text{C} \rightarrow \text{Si}_\text{C}$ ). Hence, the vacancy-interstitial complex reaction reduced the vacancies and interstitials and increased the antisites after roughly .1 - .3 ps.

Fig. 6 shows how the number of defects at the end of cascades (at 11.2 ps) produced by Si recoils varies with recoil energy at 300 K. From 5 and 50 keV, the number of point defects varied almost linearly with PKA energy. Especially, the number of C interstitials and vacancies showed larger number than other defects due to the lower displacement energies of C atoms. The number of C interstitials were greater than C vacancies because some were occupied by Si or C atoms to form  $\text{Si}_\text{C}$  or  $\text{C}_\text{C}$  antisite defects.

#### IV. CONCLUSIONS

Molecular dynamic methods were used to study defect production and evolution in 4H-SiC system. No significant dependency of displacement threshold energy on Wyckoff sites for same atoms type was recorded. For Si or C atoms, despite the difference in displacement threshold energies at various Wyckoff sites along the same crystallographic direction, their average values remained almost

similar. The average values of TDE were recorded as 66 eV for Si and 24 eV for C along 146 different crystallographic directions. Time dependence on number of point defect followed two trends. For vacancy and interstitial defect, an obvious maximum disorder peak was recorded at roughly .1 - .3 ps, and number of defects remained stable after roughly 1 ps. For antisites, the maximum disorder peak was absent, and number of antisites gradually increased then remained stable after roughly 1 ps. The energy dependence of number of stable defects that survived final stage increased almost linearly with PKA kinetic energy from 5 keV to 50 keV at 300 K. As PKA kinetic energy rose, the number of C interstitials and vacancies always showed the largest number than other defects due to lower displacement energies of C atoms.

#### ACKNOWLEDGMENTS

This work was supported by National Natural Science Fund (Grant Nos. 61575153, 61675191 and 11572054) and Longshan academic talent research supporting program of SWUST (Nos. 18LZX616).

#### REFERENCES

- P. G. Neudeck, *J. Electron. Mater.* **24**, 283–288 (1995).
- J. B. Casady and R. W. Johnson, *Solid State Electron.* **39**, 1409–1422 (1996).
- W. Bolse, *Nucl. Instrum. Methods Phys. Res. B* **148**, 83–92 (1999).
- K. Minato, K. Sawa, T. Koya, T. Tomita, A. Ishikawa, C. A. Baldwin, W. A. Gabbard, and C. M. Malone, *Nucl. Technol.* **131**, 36–47 (2000).
- J. A. Lake, R. G. Bennett, and J. F. Kotek, *Sci. Am.* **286**, 72–81 (2002).
- F. Gao, Y. Zhang, M. Posselt, and W. J. Weber, *Phys. Res. B* **74**, 104108 (2006).
- L. Giancarli, J. P. Bonal, A. Caso, G. Le Marois, N. B. Morley, and J. F. Salavy, *Fusion Eng. Des.* **41**, 165–171 (1998).
- J. C. Zink, *Power Engineering* **102**, 10 (1998).
- B. G. Kim, Y. Choi, J. W. Lee, D. S. Sohn, and G. M. Kim, *J. Nucl. Mater.* **281**, 163–170 (2000).
- R. Devanathan, W. J. Weber, and F. Gao, *J. Appl. Phys.* **90**, 2303–2309 (2001).
- R. Devanathan and W. J. Weber, *J. Nucl. Mater.* **278**, 258–265 (2000).
- S. Plimpton, *J. Comp. Phys.* **117**, 1–19 (1995).
- R. Devanathan, T. Diaz de la Rubia, and W. J. Weber, *J. Nucl. Mater.* **253**, 47–52 (1998).
- D. E. Farrell, N. Bernstein, and W. K. Liu, *J. Nucl. Mater.* **385**, 572–581 (2009).
- J. M. Bind, *Mater. Res. Bull.* **13**, 91–96 (1978).
- S. J. Zhao, J. M. Xue, C. Lan, L. X. Sun, Y. G. Wang, and S. Yan, *Nucl. Instrum. Methods Phys. Res. B* **286**, 119–123 (2012).
- W. J. Weber and F. Gao, *J. Mater. Res.* **25**, 2349–2353 (2010).
- G. D. Samolyuk, Y. N. Osetsky, and R. E. Stoller, *J. Nucl. Mater.* **465**, 83–88 (2015).
- B. S. Thomas, N. A. Marks, L. R. Corrales *et al.*, “Threshold displacement energies in rutile  $\text{TiO}_2$ : A molecular dynamics simulation study,” *Nuclear Inst & Methods in Physics Research B*, **239**(3), 191–201 (2005).
- M. Robinson, N. A. Marks, K. R. Whittle *et al.*, “Systematic calculation of threshold displacement energies: Case study in rutile,” *Physical Review B Condensed Matter* **85**(10), 104015 (2012).
- B. J. Cowen and M. El-genk, “Directional dependence of the threshold displacement energies in metal oxides,” *Modelling Simul. mater. sci. eng* **25**(8), 085009 (2017).